

Compensators for IMRT – An Investigation in Quality Assurance¹

A. Bakai, W. U. Laub, F. Nüsslin

Abt. Medizinische Physik, Radiologische Universitätsklinik, Universität Tübingen

Abstract

Intensity modulated radiotherapy (IMRT) allows dose distributions which adequately consider organs at risk (OAR) and dose homogeneity to the target volume. This is practically reached by conforming the beam profiles to the shape of the planning target volume (PTV), by shaping the fluence with multileaf collimators (MLC) or compensators. Though compensator production is time consuming and seems less convenient than the use of MLC, compensators offer much easier quality assurance. In this study the effects of certain simplifications of compensator production were studied. Compensators were produced and ionization chamber measurements in a water phantom and film measurements in a solid phantom were performed to verify the compensators. The results of the measurements were compared to the fluence distributions given by the planning system. The measurements were meant to show how realistic the investigated simplifications were, and to reveal a suitable and reliable testing method for compensators. Monte-Carlo calculations employing the EGS 4 Code were further performed to support the measurements.

Keywords: Compensators, IMRT, quality assurance

Zusammenfassung

Mit Hilfe der intensitätsmodulierten Strahlentherapie (IMRT) ist es möglich, Dosisverteilungen zu erzeugen, in denen Risikoorgane (OAR) sowie eine homogene Dosis im Zielvolumen adäquat berücksichtigt werden. Praktisch wird dies dadurch erreicht, daß die Strahlquerschnitte mittels Multi-Leaf-Kollimatoren (MLC) oder Kompensatoren an die Form des Planungszielvolumens (PTV) angepaßt werden. Obwohl die Herstellung von Kompensatoren zeitaufwendig ist und unbequemer erscheint als der Einsatz von MLC, ist hier durch die Möglichkeit einer wesentlich einfacheren Qualitätskontrolle ein entscheidender Vorteil gegeben. In dieser Arbeit wurde untersucht, welche Effekte bestimmte Vereinfachungen während der Kompensatorherstellung haben. Kompensatoren wurden angefertigt und mit ihnen zu Verifikationszwecken Messungen in verschiedenen Phantomen durchgeführt. Anschließend wurden die Meßergebnisse mit den vom Planungssystem berechneten Fluenzverteilungen verglichen. Die Messungen sollten zeigen, wie realistisch bestimmte Vereinfachungen sind und eine praktikable, zuverlässige Methode für die Qualitätskontrolle von Kompensatoren liefern. Zur Untermuerung der Messungen wurden ferner Monte-Carlo-Berechnungen mit dem EGS 4-Code durchgeführt.

Schlüsselwörter: Kompensatoren, IMRT, Qualitätssicherung

Introduction

Intensity modulated radiotherapy (IMRT) using external photon beams is a new and very promising technique since it allows dose escalation and sparing of organs at risk (OAR) [12, 14]. This becomes possible because not only the beam outlines are tailored to the shape of the planning target volume

(PTV), but also the fluence distributions across the fields are optimized. Such a 3D conformity of the irradiated volume is especially desirable if OAR are located in the immediate neighborhood of the target volume, as it is e. g. the case for tumors in the thorax.

Two main methods exist to realize intensity modulation of external beams: one is to use multileaf collimators (MLC) for

¹ This paper was partly presented at the 1999 DGMP Congress in Passau, Germany.

beam shaping, the other to install compensators in the paths of the beams [6, 12]. The latter ones are blocks made of a highly absorbing material with varying thickness according to the fluence distributions of the respective fields. While MLC allow a very elegant intensity modulation performance both in a static (Step-&Shoot) and dynamic technique (dMLC), quality assurance for MLC is simply a nightmare. Compensators, on the other side, are, particularly with regard to their production, less convenient since this process is time consuming. However, compensators offer a much easier quality assurance which is their great advantage. A high accuracy when fluence profiles are realized is naturally one of the main requirements for IMRT treatment success, and this question of accuracy can be answered much easier for compensators than for MLC [5, 6, 12, 141].

In this study the effects of certain simplifications during compensator production on measured dose distributions were investigated and compared to the original fluence distributions given by a treatment planning system. In addition to that, for all measurements also Monte-Carlo simulations were performed and compared with the results of the measurements and the calculations of the planning system. It was tried to find a method for efficient compensator testing and to find out how important such testing is. In connection with the performance of the measurements a method had to be found to calculate the monitor units (MU) from the given fluence values because standard methods for open fields cannot be used in the case of compensator modulation. The compensators used in this study belonged to a typical IMRT plan for photon radiotherapy of a target volume in the thorax. IMRT planning was done with a commercially available treatment planning system [13].

Materials and Methods

Sample Treatment Plan and Fluence Distribution Calculation with *KonRad*

For this study the inversely calculated fluence profiles of a typical IMRT treatment plan of a medium sized target volume in the thorax of an Alderson-Rando phantom were taken as basis. IMRT planning was done by means of the commercially available planning system *KonRad* (MRC Systems, Heidelberg).

For the *KonRad* calculations it is prerequisite first to specify certain volumes as OAR as well as to specify the number and directions of the treatment beams. In the present sample case the two lungs, the heart and the spinal cord were considered as OAR and for the performance of the treatment five non-coplanar beams with hand-optimized directions were chosen [7]. Based on this information, *KonRad* calculates the fluence and dose distributions by iteratively optimizing a physical target function [2, 13] – the final results are given as fluence matrices.

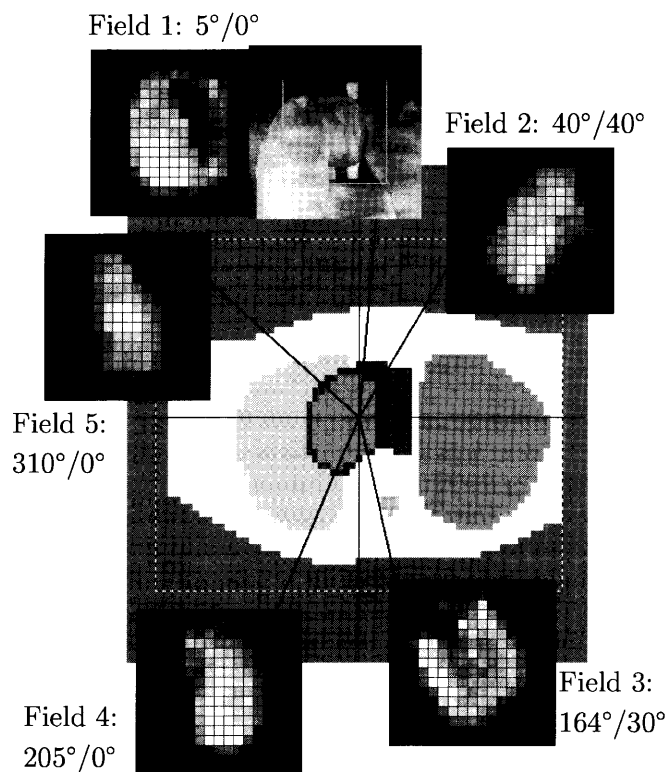


Figure 1 Transversal view of the thorax of the Alderson-Rando phantom with the target volumes and the OAR outlined. Additionally shown are the directions (by gantry angle and table rotation angle) and fluence distributions of the treatment beams and for one field the beam's-eye-view.

In Figure 1 a transversal slice of the thorax of the Alderson-Rando phantom is presented in which the target volumes and the OAR for the present case are outlined. The directions of the five beams are sketched and specified by gantry angle and rotation angle of the table around the isocenter. For all five fields the fluence distributions perpendicular to the central beam axes resulting from the calculations of the planning system are plotted and also for one of the five fields in addition to that the beam's-eye-view. For the fluence matrices ($9 \times 9 \text{ mm}^2$ pixel size) gray scale representation is used.

Experimental Verification

To generate the fluence profiles of the *KonRad* plan five compensators were produced from MCP 96. Blocks with a square base of $16 \times 16 \text{ cm}^2$ and thickness 6 cm were cast, a CNC milling machine was then used for milling the modulation profiles into the blocks. This large block thickness was needed to realize the steep fluence gradients calculated by the planning system. Since the planning system writes out fluence values for square pixels, all profiles were milled in line. However, because of the malleability of MCP 96 and the thickness of

the blocks a pre-drilling of the profiles was necessary. Remaining webs of MCP 96 between the lines after milling were removed manually. The production process per compensator took about 2 hours time.

The depths of the holes were calculated from the fluence matrices employing the exponential attenuation law for photon beams. A constant attenuation coefficient $\mu = 0.43 \text{ cm}^{-1}$ was assumed which, however, holds for monoenergetic 6 MeV photons only. This means that the photon energy spectrum was neglected which was the first simplification made in the production process. The thickness of 6 cm solid MCP 96 results in a transmission of 7.5%. Besides the neglect of the spectral energy distribution our approach included additional approximations: beam hardening as well as beam divergence and photon scattering inside of the compensator were also neglected.

For stability reasons all compensators were produced with a remaining thickness of 0.5 cm MCP 96 at their thinnest spots. The compensators were mounted on satellite plates which allowed to install them reproducibly into the beam path. When installed, the distance between focus and middle of each compensator was 64.2 cm. The idea when producing the non-focussing compensators was that the holes should have the same diameter they would have at 64.2 cm focus distance if they were produced focussed. For a spatial resolution of 9 mm in 100 cm focus distance this would have resulted in a theoretical diameter of the holes of 5.778 mm. Since common drills with 6 mm diameter were used, this discrepancy was corrected during measurement performance by scaling the focus-isocenter distance by a factor of 6/5.778.

All measurements were performed at an Elekta SL20 linear accelerator with 6 MV photons. Measurements were done in a water phantom (MP3, PTW-Freiburg) aligned parallel to the axes of the accelerator room coordinate system using a diamond detector (Type 60003, PTW-Freiburg) as field chamber and a flexible thimble chamber (Type 31002, PTW-Freiburg) as reference chamber. The diamond detector was chosen because of its excellent spatial resolution of 0.32 mm along its symmetry axis. The dependence of its response on the dose rate was corrected [8], stable response was achieved by pre-irradiating the detector before each measurement. Employing the light field and plain x - and y -profiles as well as depth dose curves the center of the sensitive volume of the diamond detector was positioned with an uncertainty of 0.1 mm which allowed a precise correlation between the measuring spot of the detector and its position.

For the verification of the compensators only measurements along the direction of the highest spatial resolution of the diamond detector were taken into account. Profile measurements were performed with 0° gantry angle and field size $15 * 15 \text{ cm}^2$. The dose profiles were acquired in dose maximum depth d_{max} , measured in 1 mm steps, the offset between adjacent profiles being 2 mm. For interesting profiles repeated scanning was done in 50 mm, 100 mm, and 200 mm depth with the same step size. Check measurements between each

compensator assured that evaporation of water or tilting of the phantom had no effect. All measuring procedures took place computer-controlled by the evaluation software of the MP3 (Mephysto Version 6.30, PTW-Freiburg).

As a second phantom for the verification of the compensators a homogeneous solid „white“ polystyrene phantom (trade name: RW3) consisting of $30 * 30 \text{ cm}^2$ slabs was employed; RW3 is water-equivalent for high energy photons [4]. To record two-dimensionally the dose deposited in this phantom CEA TVS EP films (CEA America Corporation) were used. This film was chosen because of its small intra- and inter-film sensitivity fluctuations, the vanishing energy dependence of its gradation curve, and because the optical density of this film proved to be linear with dose over a much wider range than is the case for other verification films [3].

First calibration measurements were performed. For that purpose CEA TVS EP films were positioned at the central beam axis in 9.7 cm RW3 depth (Source Skin Distance SSD = 100 cm, $10 * 10 \text{ cm}^2$ field size) and exposed in 5 MU intervals from 5 to 80 MU. The films were developed with a PROTEC machine (Type 1105, PROTEC Medizintechnik) which assured constant conditions during the developing procedure and afterwards digitized using a Vidar VXR-12 Scanner (Vidar Systems Corporation). Also non-irradiated films were scanned. The films were then analyzed with help of the Medical Imaging Software OSIRIS (University Hospital of Geneva) [1]. For each film the gray values of the nine pixels centered around the isocenter were averaged and their mean value was assumed as the gray value that results when CEA TVS EP films are irradiated with a certain number of MU. This number of pixels which corresponds to an area of approximately $1.2 * 1.2 \text{ mm}^2$ was chosen for averaging because it is large enough to average out smaller fluctuations in film sensitivity while it is at the same time small enough to avoid influence on the gray values originating from the central depression effect. In addition, an ionization chamber (Type 23331, PTW-Freiburg) was inserted into the RW3 phantom and this arrangement was irradiated under the same conditions as the films. By that it was possible to make an absolute dose calibration. A regression analysis was used for obtaining the film calibration curve.

For the compensator quality control measurements performed with films the following setup was used: for each compensator a film was positioned perpendicular to the central beam axis between 9.2 cm RW3 backscattering material and 13 mm RW3 build-up material which approximates to the dose maximum depth d_{max} in water for 6 MV photons [4]. It was taken care that equal pressure was exerted on the whole film to avoid air gaps between film and neighboring slabs [3]. For all measurements focus-film distance was 100 cm, gantry angle 0° and field size $15 * 15 \text{ cm}^2$ in analogy to the water phantom measurements. Before the irradiation of the modulated fields could take place, the number of MU had to be estimated. This number when irradiated should as completely as possible exploit the linear part of the film gradation curve

without the dose exceeding the linear dose-response of the film. By means of the central beam tables for open static fields it was assumed as a first approximation that for compensators 135 MU yield a dose of 2.0 Gy in 13 mm RW3 depth and 100 cm focus distance. This number of MU was corrected by the isocenter transmission for each field to account for the absorption by the compensators.

Dose Distribution Calculation with EGS 4

For the numerical validation of both the *KonRad* calculated and the experimentally realized fluence profiles Monte-Carlo simulations employing the EGS 4 code were performed [11]. This algorithm that is wide-spread in the area of Medical Physics was implemented in our institute into the 3D-treatment planning system VOXELPLAN (DKFZ-Heidelberg).

The Monte-Carlo simulations for this work were performed in a half-infinite homogeneous water phantom with voxels of $2.732 * 2.732 * 10 \text{ mm}^3$ size and were based on a simple accelerator head model for 6 MV photons [10, 9]. About 200 million events were simulated per field which resulted in a calculation time of about 20 h per field on a DEC Alpha 533 MHz. The *KonRad* fluence profiles were considered by assuming the number of particles coming from the accelerator head and travelling in 64.2 cm focus distance through square pixels of a plane perpendicular to the central beam axis to be proportional to the fluence values in these picture elements. For the calculations this meant infinitely thin compensators which, certainly, was a simplification. Therefore effects like scattering inside the compensators or beam hardening could not be considered. Further, the *KonRad* fluence profiles were also slightly modified: to account for the non-vanishing transmission of radiation through the compensators in areas where they have maximum thickness it was assumed that the relative fluence at each single point inside of the field borders was at least 7.5%. For all calculations a field size of $15 * 15 \text{ cm}^2$ was applied.

Results and Discussion

Calibration Curve of the CEA TVS EP Film

For the CEA TVS EP film a nearly linear dose response was found up to doses of 0.4 Gy (Figure 2). For higher dose values saturation behavior was observed due to the limited 12-bit resolution of the scanner and due to film overexposure. The result is somewhat in contradiction to the observations made by [3].

For the performance of the film quality assurance measurements in this study this result meant that the upper limit dose D_{max} that should be deposited in the films was to be chosen below 0.4 Gy. We chose $D_{max} = 0.35 \text{ Gy}$ with the intention to avoid any possible errors if our model for calculating the MU would prove to be non-satisfactory. Non-linear regression

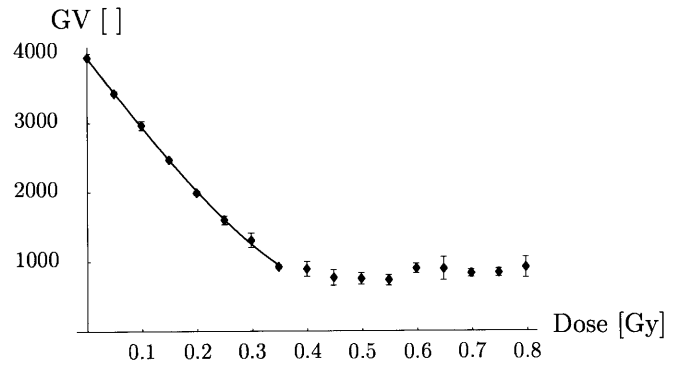


Figure 2 Calibration curve of the CEA TVS EP film (GV Gray Value).

analysis of the measured gray and dose values yielded the following expression for the film calibration curve

$$GV(D) = 12990.2 D^3 - 10150.3 D + 3936.0.$$

The equation is valid for $0 \leq D \leq 0.35$ with GV as the 12-bit gray value that belongs to a certain dose D (\overline{D} = Gy). The slope of the calibration curve is negative since the maximum gray value (4095) characterizes the white, i.e. unirradiated pixels while the other gray values down to the minimum value (0 = black) characterize irradiated film pixels. The resolution coefficient of the regression analysis proved to be $R^2 = 0.999$ and shows that the gray values are sufficiently described by this cubic equation. In the dose range suited for measurements the gray values showed a standard deviation of $\pm 50 \text{ GV}$ resulting in a dose uncertainty of $\pm 3 \%$.

Verification of the Compensators

For all five compensators measurements were performed with two aims: one was to verify the model according to which the compensators were produced, the other was simply to verify production. The measured dose distributions were therefore compared with the fluence distributions given by the planning system and the dose distributions resulting from the Monte-Carlo simulations for each field. Although dose and fluence distributions are two different entities, one may take the comparison as a clue for further statements on compensator quality.

In Figure 3 the results of diamond detector (top) and film measurement (middle) for field/compensator 1 as well as the EGS 4 calculated dose distribution (bottom) for this field are presented. All plots shown are contour plots with the 10%, 20%, ... isodose lines as contours. Each distribution is normalized to its isocenter ($x, y = 0 \text{ mm}$) value. The mere qualitative comparison of these dose distributions with the appropriate fluence distribution (s. Figure 1) already yields that the fluence distribution could in fact and at least in its main parts be generated by the compensator. Especially striking when

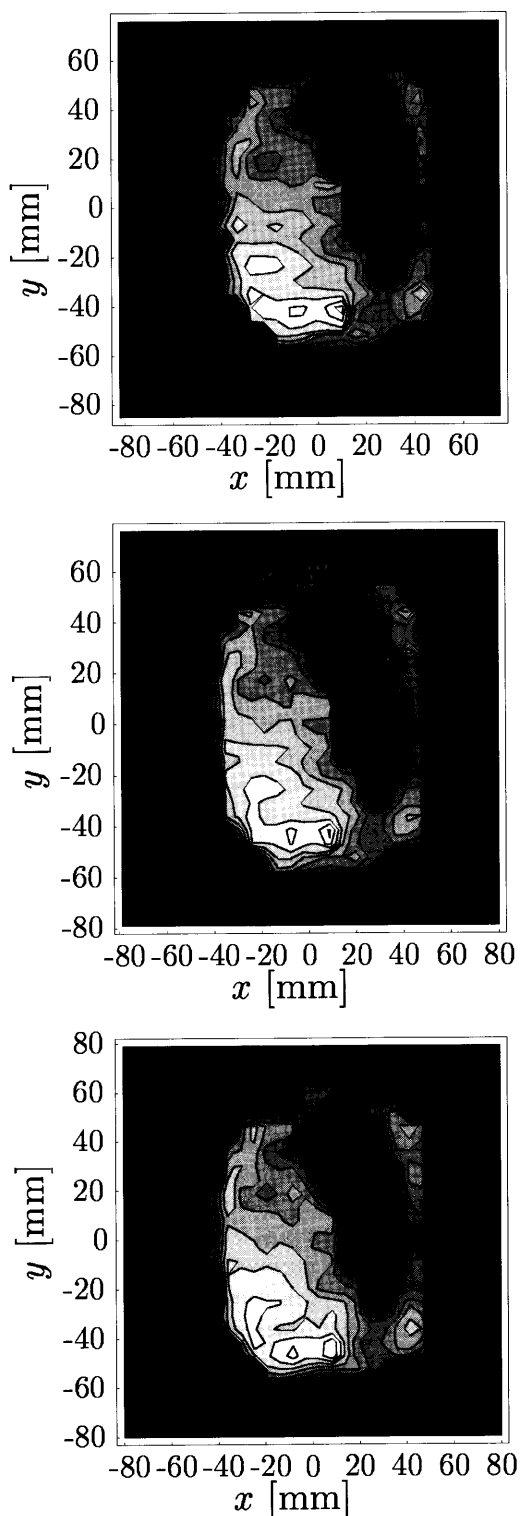


Figure 3 Field 1. Relative dose distributions resulting from diamond detector measurement (top), film measurement (middle) and EGS 4 calculation (bottom).

comparing measured dose and fluence are only the discrepancies in low intensity regions. These discrepancies can be attributed to the fact that the planning system assumed that radiation transmission through the compensator vanishes in areas where this has its maximum thickness. These discrepancies can also be demonstrated between the measured and the EGS 4 dose distribution which, apart from that, correspond qualitatively very well. Although for all Monte-Carlo simulations inside the field borders a radiation transmission through the compensator of at least 7.5% was allowed for, the real transmission was substantially higher. This was caused by the fact that the compensators were cast and not made of massive blocks. Casted blocks have a large number of small air cavities which lowers the absorption and therefore causes increased base transmission.

To make quantitative statements easier it is better to pick out single profiles from the relative distributions to compare these with each other. Figure 4 shows the dose profiles for field 1 measured with diamond detector and film in d_{max} along the line $y = 0$ mm – both profiles derived from the two-dimensional distributions. It also shows the result of the EGS 4 dose calculation along the same line and the *KonRad* fluence distribution. Further, the difference curves resulting from the EGS 4 calculation and the diamond detector measurement and from EGS 4 and the film measurement are plotted. As before, $x = 0$ mm corresponds to the isocenter. As could be presumed from Figure 3 it is by and large possible to verify the measured profiles on the fluence distribution of the field if one takes into account the uncertainties when performing the measurements (inaccuracies in detector positioning, film calibration curve uncertainties, ...) and the inaccuracies when manufacturing the compensators (remaining MCP 96 webs, non-focussing production, ...). However, there are also some larger discrepancies. These occur in high intensity regions and near steep dose gradients: the measured profiles as well as the EGS 4 dose profile are smeared compared to the *KonRad* fluence profile. This smearing is caused by scattering inside the compensator and inside water and RW3, respectively. The fact that scattering inside the compensator was also not taken into account in the Monte-Carlo calculations explains to some extent the slight differences ($\leq 3\%$) between the experimentally determined distributions and the Monte-Carlo profile in high intensity regions. Scattering in the compensator should therefore be part of EGS 4 for future simulations. Another reason for the discrepancies between the results of the measurements and the EGS 4 result is the finite size of the voxels in which dose values were averaged. From Figure 4 one can extract the minimum radiation transmission through the compensator which was at least partially considered when performing the Monte-Carlo simulations. So in the low intensity regions the actual dose which traces back to the base transmission amounts to approximately 25% of the isocenter dose value. If this is seen relative to the maximum measured dose it corresponds to a transmission of approximately 17% which is much more than the considered 7.5%.

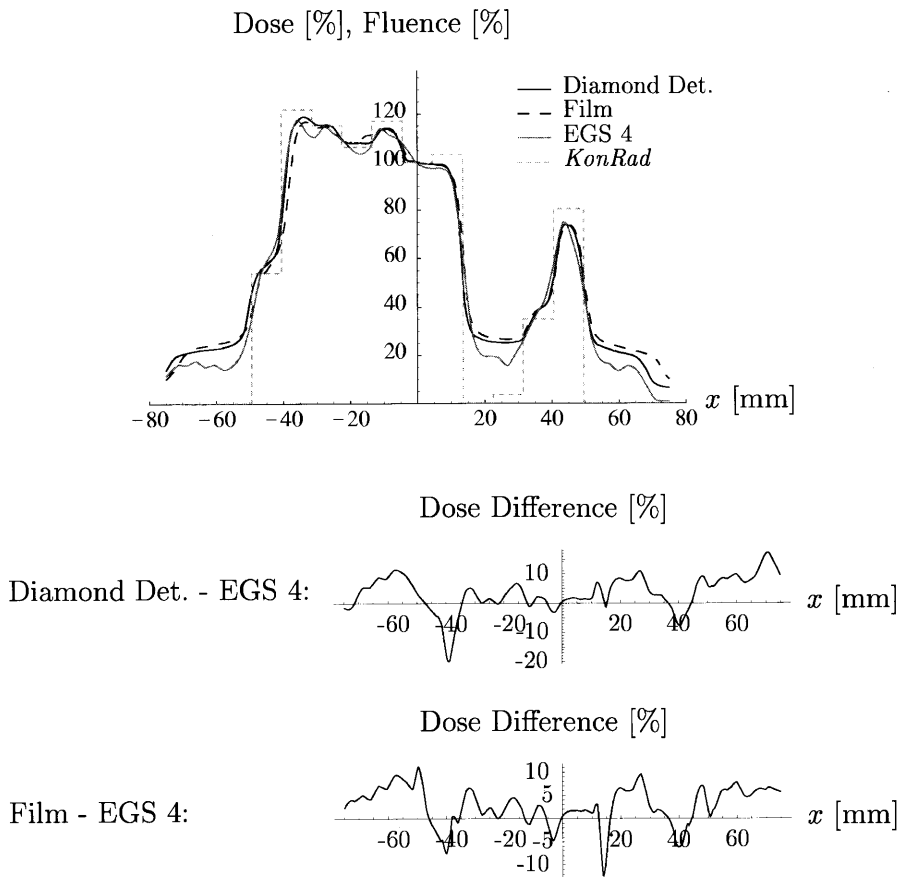


Figure 4 Field 1. Dose profiles measured with diamond detector and film along $y = 0$ mm in d_{max} , the result of the corresponding EGS 4 calculation and the given fluence distribution. The two additional graphs below illustrate the difference between EGS 4 calculation and diamond detector or film measurement.

As shown in Figure 4 diamond detector and film measurement are in good agreement. The deviations of $\leq 2.5\%$ are within the scope of the measuring uncertainties. Larger deviations between the measured dose distributions occur only locally near steep gradients and are due to the differences in spatial resolution between the two measuring methods. Since similar results were also found for other offsets and for the other compensators the very good agreement between the two measuring methods leads to the conclusion that film measurements which can be performed much more conveniently are sufficient for quality control of IMRT compensators.

To allow an even more solid comparison between measurements and EGS 4 dose calculations, for interesting profiles diamond detector measurements from various depths were compared to the results of simulations performed in these depths. Such profiles are presented in Figure 5 for field 1. All profiles shown in this figure belong to the y -offset = -14.0 mm and are normalized to the maxima of the 15 mm curves. The solid curves represent the measurements, the dashed curves the results of the Monte-Carlo calculations. The figure also contains two more graphs which describe the difference between measurement and Monte-Carlo simulation in 15 mm and 200 mm depth. The comparison of the two 15 mm curves confirms – if one does not take low intensity regions into account – the formerly seen discrepancies of on the average $\leq 3\%$ caused by uncertainties du-

ring compensator manufacturing and by the neglect of scatter inside the compensator in the EGS 4 calculations. In this context one should mention the MCP 96 webs or spots that could not be removed from the compensators during production and which reached heights up to 3 mm. These spots can be identified in the measured dose distributions due to the excellent spatial resolution of the diamond detector since they lead to cold dose spots ($\leq 5\%$) as observed for instance at $x = 15$ mm in the diamond detector profile. It is important to take care that the number of remaining webs is as low as possible.

The approximation of producing non-focussed compensators had no substantial impact on the dose distribution. For example, comparing the dose values at 15 mm depth at the two coordinates $x = -50$ mm and $x = 15$ mm where the steepest dose gradients are located, one can see that although these two points have different isocenter distances, there is no substantial difference between measurement and calculation between the two points. The width of the profiles gets larger with larger depth due to the divergence of the radiation beam. But also in these depths measurements and calculations correspond very well. The discrepancies even get smaller due to photon scattering in water as can be seen in the difference curve for 200 mm depth. Equal results were found for other offsets. The good agreement between measurements and Monte-Carlo calculations in different depths shows that

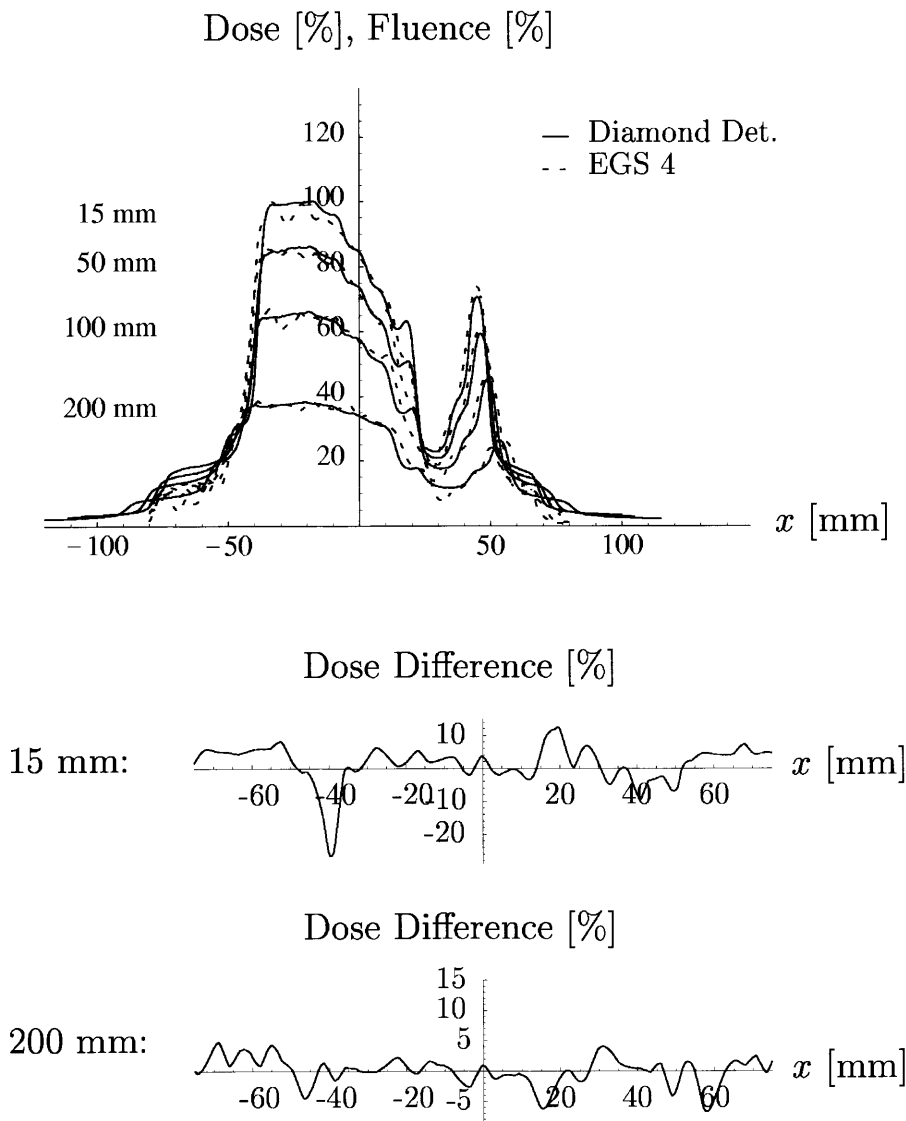


Figure 5 Field 1. Measured and EGS 4 calculated dose profiles from various depths belonging to $y = -14.0$ mm. The additional graphs below illustrate the differences between measurement and Monte-Carlo calculation in 15 mm and 200 mm depth, respectively.

neglecting beam hardening in the calculations has no essential effect on the dose distribution. The same is true for scattering inside the compensator. It was therefore possible by employing a simple compensator model to manufacture a compensator which indeed produced the given fluence distribution with a high accuracy.

The measurements, calculations and simulations performed for the four other fields, and especially the comparisons of these yielded similar results to that of field 1 which were presented here. Therefore a presentation of these fields was omitted.

Another aim of the measurements was to check the compensators for mistakes during production. When comparing measured dose distributions and fluence distributions it was found in some cases that compensators and satellite plates were misaligned. This observation proved that production mistakes can easily occur and that they definitely have to be taken into account.

Conclusions

This study showed that it was possible to realize the fluence profiles of a sample treatment plan employing the simple compensator model proposed here. It was in all main parts possible to verify the compensator modulated dose distributions within the measuring uncertainties and the inaccuracies that accompanied compensator production on the respective fluence distributions. Larger discrepancies between measured dose values and fluence values occurred only in low intensity regions, where the treatment planning system did not take base transmission into account, and near steep fluence gradients. Steep fluence gradients are critical because they are difficult to realize and should therefore be avoided. A welcome side effect of flatter fluence profiles would be that compensators could be much thinner and therefore be lighter which would make their usage in every day's clinical routine

practicable. Also the compensator production itself would become more convenient. And flatter fluence profiles would yield in a reduction of the sensitivity of compensators for positioning errors which limit treatment success.

The good agreement (deviations $\leq 3\%$) between diamond detector and film measurements showed that film measurements are indeed sufficient for compensator quality checking. One is not allowed to dispense with such quality assurance measurements, if one wants to exclude with certainty any possible error during compensator production.

Between measurements and Monte-Carlo simulations also in all main field parts a very good agreement (discrepancies $\leq 5\%$) was found. The fact that the compensators were produced non-focussing and that the simulations did not take into account beam hardening and scattering inside the compensators lead to no relevant deviations.

It now remains to be investigated with what accuracy dose distributions can be produced with these compensators in the Alderson-Rando phantom to which the investigated treatment plan belongs and, by that, how feasible IMRT in the thorax under actual circumstances really is.

Acknowledgements

The authors would like to thank MRC Systems Heidelberg for placing the treatment planning system *KonRad* at their disposal.

This work was supported in part by the Deutsche Krebs-hilfe.

References

- [1] Bakai, A.: *Qualitätssicherung bei intensitätsmodulierter Bestrahlung im Thoraxbereich*. Diplomarbeit, Universität Tübingen 1999
- [2] Bortfeld, T., Stein, J., Preiser, K.: *Clinically relevant intensity modulation using physical criteria*. In: Leavitt, D. D., Starkshall, G. (Eds.) Proceedings of the XIIth International Conference on the Use of Computers in Radiation Therapy, Salt Lake City, UT, USA. Medical Physics Publishing, 1997, pp. 1–4
- [3] Cheng, C.-W., Das, I. J.: *Dosimetry of high energy photon and electron beams with CEA films*. Med. Phys. **23** (1996) 1225–1232
- [4] Christ, G.: *White polystyrene as a substitute for water in high energy photon dosimetry*. Med. Phys. **22** (1995) 2097–2100
- [5] Convery, D. J., Rosenbloom, M. E.: *Treatment Delivery Accuracy in Intensity Modulated Conformal Radiotherapy*. Phys. Med. Biol. **40** (1995) 979–999
- [6] Helbig, A.: *Dosimetrische Verifikation intensitätsmodulierter Photonenbestrahlungen in der Tumorthherapie*. Diplomarbeit, Deutsches Krebsforschungszentrum Heidelberg 1998
- [7] Kistler, S.: *Richtungsoptimierung intensitätsmodulierter Felder bei Konformationstherapie von Tumoren mit hochenergetischer Photonenstrahlung*. Diplomarbeit, Universität Tübingen 1999
- [8] Laub, W. U., Kaulich, T. W., Nüsslin, F.: *Energy and Dose Rate Dependence of a Diamond Detector in the Dosimetry of 4-25 MV Photon Beams*. Med. Phys. **24** (1997) 535–536
- [9] Laub, W. U., Alber, M., Birkner, M., Nüsslin, F.: *Monte Carlo dose computation for IMRT optimization*. Phys. Med. Biol. **45** (2000, No.7) 1741–1754
- [10] Laub, W. U., Huber, B., Nüsslin, F.: *Verifikation der Berechnung von Dosisverteilungen in der 3D-Bestrahlungsplanung mit Photonenstrahlung durch Monte-Carlo Simulationen*. In: Voigtmann, L. (Ed.): Medizinische Physik, 1998, p. 39
- [11] Nelson, W. R., Hirayama, H., Rogers, D. W. O.: *The EGS 4 Code System*. SLAC Report-265 (1985)
- [12] Schlegel, W., Kneschaurek, P.: *Inverse Bestrahlungsplanung*. Strahlenther. Onkol. **175** (1999) 197–207
- [13] Schulze, C., Pijpelink, J. et al.: *3D Photon Dose Calculation: From a Scientific Tool to Routine Planning*. In: Leavitt, D. D., Starkshall, G. (Eds.): Proceedings of the XIIth International Conference on the Use of Computers in Radiation Therapy, Salt Lake City, UT, USA. Medical Physics Publishing, 1997, pp. 43–45
- [14] Webb, S.: *The Physics of Conformal Radiotherapy: Advances in Technology*. IOP Publishing. Bristol 1997

Received 11. 09. 2000; accepted for publication 15. 01. 2000.

Correspondence to:

Annemarie Bakai
Abt. Medizinische Physik
Radiologische Universitätsklinik
Universität Tübingen
Hoppe-Seyler-Str. 3
D-72076 Tübingen